

# Shear band spacing in gradient-dependent thermoviscoplastic materials

R. C. Batra, L. Chen

8

**Abstract** We study thermomechanical deformations of a viscoplastic body deformed in simple shear. The strain gradients are taken as independent kinematic variables and the corresponding higher order stresses are included in the balance laws, and the equation for the yield surface. Three different functional relationships, the power law, and those proposed by Wright and Batra, and Johnson and Cook are used to relate the effective strain rate to the effective stress and temperature. Effects of strain hardening of the material and elastic deformations are neglected. The homogeneous solution of the problem is perturbed and the stability of the problem linear in the perturbation variables is studied. Following Wright and Ockendon's postulate that the wavelength whose initial growth rate is maximum determines the minimum spacing between adjacent shear bands, the shear band spacing is computed. It is found that the minimum shear band spacing is very sensitive to the thermal softening coefficient/exponent, the material characteristic length and the nominal strain-rate. Approximate analytical expressions for the critical wavelength for heat conducting nonpolar materials and locally adiabatic deformations of gradient dependent materials are also derived.

**Keywords:** Material characteristic length, strain-rate gradient, dominant growth rate, viscoplastic material, stability

## 1 Introduction

Most of the analytical, numerical and experimental studies on adiabatic shear bands have focussed on analyzing the initiation and growth of a single shear band; e.g. see the book by Bai and Dodd (1992), the review article by Tomita (1994), papers in a special issue of *Mechanics of Materials* edited by Armstrong et al. (1994), the volume edited by Batra and Zbib (1994), and the book edited by Perzyna

(1998). Batra (1987), Batra and Kim (1990a), and Kwon and Batra (1988) have numerically studied the interaction among shear bands in a thermo-elasto-viscoplastic body deformed in simple shear. They perturbed the solution of the nonlinear coupled partial differential equations governing the deformations of the body by introducing a temperature perturbation with multiple cusps and numerically solved the resulting nonlinear problem to see if one or more shear bands formed. Kwon and Batra found that for a typical steel modeled as a nonpolar (simple) material, a shear band formed at each trough in the cosine wave in a specimen deformed at an overall strain-rate of 500/s but at each crest when the nominal strain-rate equalled 50,000/s. For dipolar materials with material characteristic length equal to 0.5% of the specimen thickness, at a nominal strain-rate of 500/s a shear band formed only at the two bounding surfaces where the velocity was prescribed and at each crest when the nominal strain-rate was 50,000/s. Both for dipolar and nonpolar materials deformed at an average strain-rate of 50,000/s, the distance between adjacent shear bands was found to be 0.258 mm. They did not attempt to find the minimum spacing between shear bands. Similarly, Batra and Liu (1990) and Batra and Hwang (1994) studied the interaction among shear bands formed in a thermoviscoplastic body deformed in plane strain compression but did not find the minimum spacing between shear bands.

Grady and Kipp (1987) obtained the minimum shear band spacing by accounting for momentum diffusion due to unloading within bands. Wright and Ockendon (1996) considered simple shearing deformations of a thermoviscoplastic block, perturbed the homogeneous solution of the governing equations, derived equations linear in the amplitude of the perturbations and thus studied the stability of the homogeneous solution. They postulated that perturbations growing simultaneously at different sites will never merge and thus result in multiple shear bands. Hence the wavelength of the mode with the maximum initial growth rate corresponds to the minimum spacing between shear bands. Wright and Ockendon neglected the effect of strain hardening of the material, and also of the boundary conditions imposed at the edges of the block. Molinari (1997) has generalized Wright and Ockendon's work to strain hardening materials, has characterized the effect of strain hardening exponent on the minimum shear band spacing, and has delineated the error in the minimum shear band spacing caused by the finite thickness of the block.

Nesterenko et al. (1995) observed multiple shear bands during the radial collapse of an explosively loaded thick-

*Communicated by S. N. Atluri, 20 September 1998*

R. C. Batra, L. Chen  
Virginia Polytechnic Institute and State University,  
Department of Engineering Science and Mechanics,  
MC-0219, Blacksburg, VA 24061, USA

*Correspondence to:* R. C. Batra

This work was partially supported by the NSF grant 9411343, ONR grant N00014-98-1-0300 and the ARO grant DAAH04-95-1-0042 to Virginia Polytechnic Institute and State University.

walled cylinder. Shear bands were observed to emanate from the inner boundary of the cylinder with regular spacing between the bands. For both austenitic stainless steel and titanium cylinders, the spacing between shear bands was found to be about 1 mm.

Wright and Batra (1987) observed that strain gradients across a shear band are extremely high and generalized Green et al.'s (1968) work for dipolar elastic-plastic materials to simple shearing deformations of dipolar elastic-viscoplastic materials. They considered the strain gradient as a kinematic variable and the corresponding higher-order stress a kinetic variable. The dipolar (i.e. strain gradients) effects stabilize deformations of the body, delay the onset of shear bands, regularize the problem, and eliminate the dependence of results upon the finite element mesh used. Batra and Hwang (1993) have generalized the one-dimensional dipolar theory of Wright and Batra (1987) to three-dimensional problems. Here we extend Wright and Ockendon's work on shear band spacing to gradient-dependent materials deformed in simple shear. Three different material models, viz., the power law, the Wright-Batra relation, and the Johnson-Cook expression are used to represent the thermoviscoplastic response of the material. For high strain-rates, the power law and the Wright-Batra relation differ essentially in the way thermal softening is accounted for, and the Wright-Batra and Johnson-Cook relations in the way strain-rate hardening is considered. For each material model, the homogeneous solution of the governing equations exhibits softening behavior at time  $t = 0$ . That is, the stress is maximum at  $t = 0$ . The initial growth rate of the perturbation depends upon the wave number and the time  $t_0$  when the perturbation is introduced. When thermal softening is modeled by an affine function of temperature, the maximum value of the wave number of the perturbation corresponding to the dominant initial growth rate of the perturbation occurs for a large value of  $t_0$ . However, for the thermal softening modeled by the power law, the wave number of the perturbation that initially grows fastest is largest for  $t_0 = 0$ . For each material model, the minimum shear band spacing depends strongly upon the strain-rate hardening exponent/parameter, material characteristic length, and the thermal softening coefficient/exponent.

## 2

### Formulation of the problem

We study thermomechanical deformations of a layer of thickness  $2H$  in the  $y$ -direction, extending to infinity in the other two directions, and being sheared in the  $x$ -direction. In terms of nondimensional variables (Batra and Kim (1990a)), the governing equations are

$$\rho \dot{v} = (s - \ell \sigma_{,y})_{,y}, \quad (1)$$

$$\dot{\theta} = k \theta_{,yy} + s \dot{\gamma} + \ell \sigma \dot{d}, \quad (2)$$

$$\dot{\gamma} = v_{,y}, \quad \dot{d} = v_{,yy}, \quad (3)$$

$$s = \Lambda v_{,y}, \quad \sigma = \Lambda v_{,yy} / \ell, \quad (4)$$

$$I \equiv (\dot{\gamma}^2 + \ell^2 \dot{d}^2)^{1/2} = f(s, \sigma, \theta). \quad (5)$$

Here  $\rho$  is the mass density,  $v$  the velocity,  $s$  the shear stress,  $\ell$  a material characteristic length,  $\sigma$  the dipolar

stress corresponding to the strain-rate gradient  $v_{,yy}$ ,  $\theta$  the temperature rise,  $k$  the thermal conductivity, a comma followed by  $y$  signifies partial differentiation with respect to  $y$ , a superimposed dot indicates the material time derivative, and  $\Lambda$  is the plastic multiplier. Equations (1) and (2) express respectively the balance of linear momentum and the balance of internal energy, and Eqs. (4) and (5) are constitutive relations. Here we have neglected elastic deformations and assumed that all of plastic working is converted into heating. Equations (4)<sub>1</sub> and (4)<sub>2</sub> imply that

$$s v_{,yy} = \sigma \ell v_{,y}. \quad (6)$$

Governing equations for nonpolar materials are obtained from (1), (2) and (5) by setting  $\ell = 0$ . The nondimensional variables are related to their dimensional counterparts, indicated by a superimposed bar, as follows.

$$\begin{aligned} \bar{y} &= Hy, & \bar{\ell} &= H\ell, & \bar{\gamma} &= \gamma, & \bar{d} &= d/H, \\ \bar{s} &= s_0 s, & \bar{\sigma} &= s_0 H \ell \sigma, & \bar{t} &= t / \dot{\gamma}_0, & \bar{\theta} &= \theta \theta_0, \\ \bar{\rho} H^2 \dot{\gamma}_0^2 / s_0 &= \rho, & \bar{k} / \bar{\rho} \bar{c} \dot{\gamma}_0 H^2 &= k, & \theta_0 &\equiv s_0 / \bar{\rho} \bar{c}. \end{aligned} \quad (7)$$

Here  $s_0$  is the yield stress in a quasistatic simple shear test,  $\dot{\gamma}_0$  the average strain-rate, and  $\bar{c}$  the specific heat.

We presume that overall deformations of the layer are adiabatic, and deformations are driven by nondimensional shearing speeds  $\pm 1 (= \bar{v}_0 / \dot{\gamma}_0 H)$  prescribed at the upper and lower bounding surfaces. That is,

$$\theta_{,y}|_{y=\pm 1} = 0, \quad v|_{y=\pm 1} = \pm 1. \quad (8)$$

We neglect the effect of strain hardening and consider three different forms for the function  $f$  in Eq. (5); the Wright-Batra (WB) relation (1987), the power law (e.g. see Molinari (1997)), and the Johnson-Cook relation (1983). These may be written as

$$f(s, \sigma, \theta) = \frac{1}{b} \left[ \left( \frac{(s^2 + \sigma^2)^{1/2}}{(1 - \alpha \theta)} \right)^{1/m} - 1 \right] \quad (9a)$$

for the WB relation,

$$f(s, \sigma, \theta) = \mu_0^{-1/m} (s^2 + \sigma^2)^{1/2m} \theta^{-v/m} \quad (9b)$$

for the power law, and

$$f(s, \sigma, \theta) = \dot{\gamma}_* \exp \left\{ \frac{1}{C} \frac{(s^2 + \sigma^2)^{1/2}}{(1 - \alpha \theta)} - 1 \right\} \quad (9c)$$

for the Johnson-Cook relation. In (9a)  $\alpha (= \bar{\alpha} \theta_0)$  is the coefficient of thermal softening, and parameters  $b (= \bar{b} \dot{\gamma}_0)$  and  $m$  characterize the strain-rate hardening of the material. For moderate to high strain-rates,  $bI \gg 1$  and  $(1 + bI)^m \simeq b^m I^m$  with the exponent  $m \ll 1$ . In (9b)  $m$  characterizes the strain-rate hardening of the material,  $v (< 0)$  its thermal softening and  $\mu_0 (= \bar{\mu}_0 \dot{\gamma}_0^m s_0^{v-1} / (\bar{\rho} \bar{c})^v)$  is related to the yield stress of the material. In (9c),  $\alpha$  is the coefficient of thermal softening,  $\dot{\gamma}_* (= \bar{\dot{\gamma}}_* / \dot{\gamma}_0)$  is a reference strain-rate, and  $C$  characterizes the strain-rate hardening of the material.

An homogeneous solution of Eqs. (1)–(3), (5), (6), (8) and (9a) is

$$\tilde{\mathbf{s}}^0 = \begin{Bmatrix} \tilde{v}^0 \\ \tilde{s}^0 \\ \tilde{\sigma}^0 \\ \tilde{\theta}^0 \end{Bmatrix} = \begin{Bmatrix} y \\ (\Gamma e^{-\Gamma t})/\alpha \\ 0 \\ (1 - e^{-\Gamma t})/\alpha \end{Bmatrix} \quad (10a)$$

where  $\Gamma = \alpha b^m$ , that of (1)–(3), (5), (6), (8) and (9b) is

$$\tilde{\mathbf{s}}^0 = \begin{Bmatrix} y \\ \mu_0(\theta^0)^v \\ 0 \\ (\theta_i^{1-v} + (1-v)\mu_0 t)^{1/(1-v)} \end{Bmatrix} \quad (10b)$$

where  $\theta_i$  is the temperature at time  $t = 0$ , and that of (1)–(3), (5), (6), (8) and (9c) is

$$\tilde{\mathbf{s}}^0 = \begin{Bmatrix} y \\ A \exp(-A\alpha t) \\ 0 \\ (1 - \exp(-A\alpha t))/\alpha \end{Bmatrix} \quad (10c)$$

where  $A = (1 - C \ln \dot{\gamma}_*)$ . Note that  $\tilde{\mathbf{s}}^0$  is non-dimensional.

### 3

#### Perturbation analysis

We perturb the homogeneous solution at time  $t_0$  by an infinitesimal amount

$$\delta \mathbf{s}(y, t, t_0) = e^{\eta(t-t_0) + i\xi y} \delta \mathbf{s}^0 \quad (11)$$

where

$$\delta \mathbf{s}(y, t, t_0) = [\delta v(y, t), \delta s(y, t), \delta \sigma(y, t), \delta \theta(y, t)]^T, t \geq t_0, \quad (12)$$

$$\delta \mathbf{s}^0 = [\delta v^0, \delta s^0, \delta \sigma^0, \delta \theta^0]^T, \quad (13)$$

$\delta s^0$  is infinitesimal amplitude of the perturbation,  $\xi$  the wave number, and  $\eta$  the initial growth rate of the perturbation. The homogeneous solution  $\tilde{\mathbf{s}}^0$  is stable or unstable according as  $\text{Re}(\eta) < 0$  or  $\text{Re}(\eta) > 0$ .

Substitution of the perturbed solution

$$\mathbf{s}(y, t, t_0) = \tilde{\mathbf{s}}^0(y, t) + \delta \mathbf{s}(y, t, t_0) \quad (14)$$

into the governing Eqs. (1), (2), (5) and (6), and linearization yields

$$\mathbf{A}(t_0, \eta, \xi) \delta \mathbf{s}^0 = 0 \quad (15)$$

where

$$\mathbf{A}(t_0, \eta, \xi) = \begin{bmatrix} \rho\eta & -i\xi & -\ell\xi^2 & 0 \\ -is^0\xi & -1 & 0 & \eta + k\xi^2 \\ -\ell s^0\xi^2 & 0 & -1 & 0 \\ i\xi & -f_{,s}^0 & -f_{,\sigma}^0 & -f_{,\theta}^0 \end{bmatrix}, \quad (16)$$

$f_{,s}^0 = (\partial f / \partial s)|_{\mathbf{s} = \mathbf{s}^0}$  etc. and the superscript zero signifies the value of the quantity at time  $t_0$ . In order for Eq. (15) to have a nontrivial solution for  $\delta \mathbf{s}^0$ ,  $\det \mathbf{A} = 0$  which gives

$$a_2 \eta^2 + a_1 \eta + a_0 = 0 \quad (17)$$

where

$$\begin{aligned} a_2(t_0) &= -\rho f_{,s}^0, \\ a_1(\xi, t_0) &= -\ell^2 s^0 f_{,s}^0 \xi^4 - (1 + \rho k f_{,s}^0) \xi^2 - \rho f_{,\theta}^0, \\ a_0(\xi, t_0) &= -\ell^2 k s^0 f_{,s}^0 \xi^6 - (k + \ell^2 s^0 f_{,\sigma}^0) \xi^4 + s^0 f_{,\theta}^0 \xi^2. \end{aligned} \quad (18)$$

For the choice (9a) of the function  $f$  and recalling that  $bI \gg 1$  so that  $(1 + bI)^m \simeq b^m I^m$ , relations (18) simplify to the following.

$$\begin{aligned} a_2(t_0) &= -\rho e^{\Gamma t_0} / (mb^m), \\ a_1(\xi, t_0) &= -\ell^2 \xi^4 / m - (1 + \rho k e^{\Gamma t_0} / (mb^m)) \xi^2 \\ &\quad - (\rho \alpha e^{\Gamma t_0}) / m, \end{aligned} \quad (19a)$$

$$a_0(\xi, t_0) = -\ell^2 k \xi^6 / m - (k + \ell^2 \alpha b^m / m) \xi^4 + \alpha b^m \xi^2 / m.$$

When the function  $f$  is given by (9b), relations (18) become

$$\begin{aligned} a_2(t_0) &= -\frac{\rho}{m\mu_0} (\theta^0)^{-v}, \\ a_1(\xi, t_0) &= \frac{-\ell^2}{m} \xi^4 - \left(1 + \frac{\rho k}{m\mu_0} (\theta^0)^{-v}\right) \xi^2 + \frac{\rho v}{\theta^0 m}, \\ a_0(\xi, t_0) &= \frac{-\ell^2 k}{m} \xi^6 - \left(k - \frac{\ell^2 v \mu_0}{m} (\theta^0)^{v-1}\right) \xi^4 \\ &\quad - \frac{v \mu_0}{m} (\theta^0)^{v-1} \xi^2 \end{aligned} \quad (19b)$$

For the function  $f$  given by (9c), relations (18) simplify to

$$\begin{aligned} a_2(t_0) &= -\frac{\rho}{C} e^{\alpha A t}, \\ a_1(\xi, t_0) &= -\frac{\ell^2 A}{C} \xi^4 - \left(1 + \frac{\rho k}{C} e^{\alpha A t}\right) \xi^2 - \frac{\rho \alpha A}{C} e^{\alpha A t}, \\ a_0(\xi, t_0) &= -\frac{\ell^2 k A}{C} \xi^6 - \left(k + \ell^2 \frac{\alpha A^2}{C}\right) \xi^4 + \frac{\alpha A^2}{C} \xi^2 \end{aligned} \quad (19c)$$

For a wave number  $\xi$  compatible with boundary conditions, equation (17) will have two roots. The instability of the homogeneous solution is governed by the root with the larger positive real part; this can be determined numerically and is hereafter referred to as the initial dominant growth rate. Results presented below are for a plate of infinite thickness; thus the effect of boundary conditions has been neglected.

Results are computed for the titanium studied by Molinari (1997), SAE4340 steel studied by Batra and Kim (1990b), and a S-7 tool steel.

#### 3.1

##### Results for Titanium modeled by the power law

The material was modeled by the power law, and parameters were assigned the following values in SI units given by Molinari (1997).

$$\begin{aligned} \bar{\rho} &= 4510 \text{ kg/m}^3, & \bar{c} &= 528 \text{ J/kg}^\circ\text{C}, & \bar{k} &= 19 \text{ W/m}^\circ\text{C}, \\ \dot{\gamma}_0 &= 10^4 / \text{s}, & s_0 &= 405 \text{ MPa}, & \bar{\theta}_i &= 300 \text{ K}, \\ H &= 2.5 \text{ mm}, & m &= 0.033, & v &= -1.7, \\ \ell &= 0.001, & \bar{\mu}_0 &= 12 \times 10^{12}. \end{aligned} \quad (20)$$

The value of  $H$  is used to non-dimensionalize quantities. With strain-hardening neglected, the stress begins to decrease right from the beginning. Figure 1 depicts, for different values of the time  $t_0$  when the perturbation is introduced, the dependence of the initial dominant growth rate  $\eta$  of the perturbation upon the wave number. It is

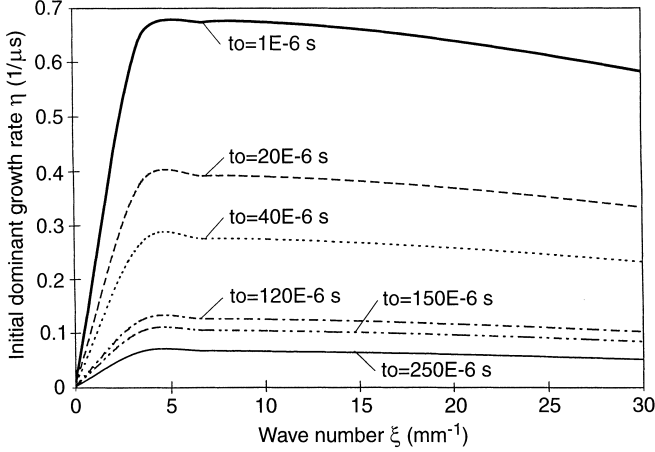


**Fig. 1.** Variation of the initial dominant growth rate vs. the wave number of the perturbation for six different values of the time  $t_0$  when the perturbation is introduced. Results are for a titanium alloy modeled by the power law

evident that for a given value of  $t_0$ , the initial dominant growth rate of the perturbation depends upon the wave number; it first increases with an increase in the wave number  $\xi$ , reaches a maximum and then decreases with an increase in  $\xi$ . We henceforth denote the maximum dominant initial growth rate by  $\eta_m$ , the corresponding wave number by  $\xi_m$ , and call  $\eta_m$  and  $\xi_m$  the critical growth rate and the critical wave number respectively; both  $\eta_m$  and  $\xi_m$  depend upon  $t_0$ . Figures 2a and 2b exhibit respectively the dependence of  $\eta_m$  and  $\xi_m$  upon  $t_0$  for material characteristic length  $\ell = 0, 0.001, 0.005$  and  $0.01$ . For each value of  $\ell$  considered,  $\eta_m$  decreases exponentially with an increase in  $t_0$ , and  $\xi_m^{-1}$  increases gradually with  $t_0$ . The  $\eta_m$  vs.  $t_0$  and  $\xi_m^{-1}$  vs.  $t_0$  curves are similar for each value of  $\ell$ . As the value of  $\ell$  is increased from 0 to 0.01 at a fixed  $t_0$ , the critical wavelength increases and the critical growth rate decreases. When strain hardening effects are considered, the  $\eta_m$  vs.  $t_0$  and  $\xi_m^{-1}$  vs.  $t_0$  curves do not change monotonically but exhibit a local maxima and minima at possibly different values of  $t_0$  (e.g. see Molinari (1997)). For the problem studied here with no strain hardening,  $\eta_m$  and  $\xi_m^{-1}$  assume their maximum and minimum values at  $t_0 = 0$ .

Wright and Ockendon (1996) postulated that the minimum spacing,  $L_s$ , between adjacent shear bands is determined by the critical wave number  $\xi_m$ . Thus

$$L_s = \frac{2\pi}{\xi_m(t_0)} \quad (21)$$

gives the minimum shear band spacing, henceforth we refer to  $L_s$  simply as shear band spacing. Here  $t_0^\eta$  corresponds to the time when  $\eta_m(t_0)$  is maximum. Molinari (1997) found that for strain hardening materials described by a power law  $\eta_m$  and  $\xi_m$  assume their maximum values at about the same value of time  $t_0$ , and computed results by using the following relation

$$L_s = \inf_{t_0 \geq 0} \frac{2\pi}{\xi_m(t_0)} \quad (22)$$

For power law type constitutive relation, Eqs. (21) and (22) give essentially the same value of the shear band spacing.

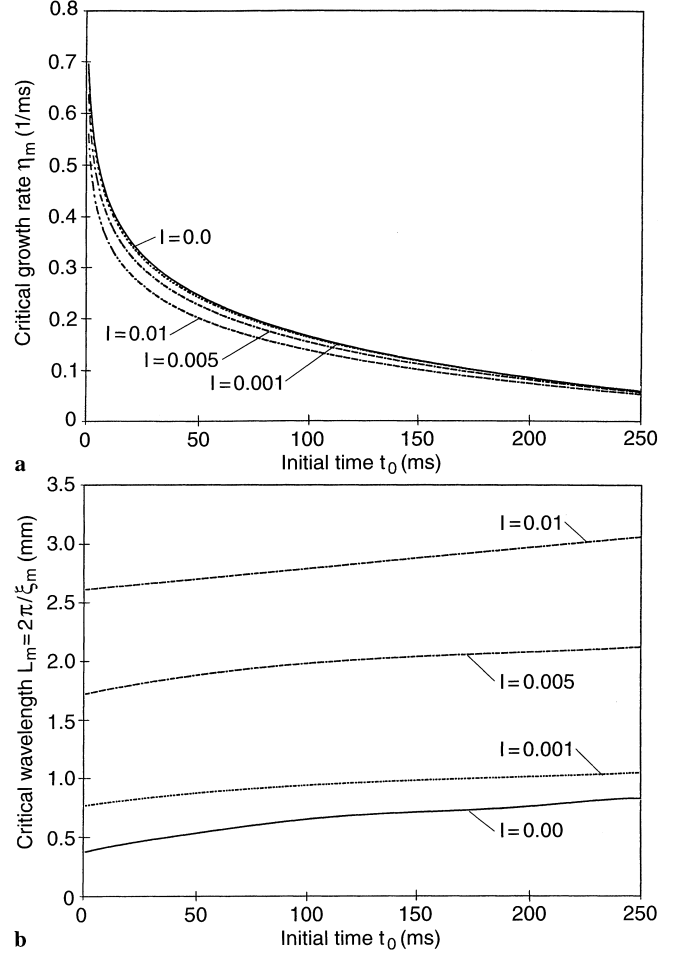


**Fig. 2.** Critical growth rate  $\eta_m$  and the critical wavelength  $L_m$  vs.  $t_0$  for four different values of the material characteristic length  $\ell$ . Results are for a titanium alloy modeled by the power law

However, for the thermal softening described by an affine function, results obtained from (21) and (22) are quite different. Results presented below are computed with Eq. (22).

Figures 3, 4, 5, 6 and 7 respectively exhibit the dependence of  $L_s$  and the maximum critical growth rate upon the material characteristic length  $\ell$ , thermal conductivity  $k$ , strain-rate hardening exponent  $m$ , thermal softening exponent  $\nu$ , and the nominal strain-rate  $\dot{\gamma}_0$ . In each case, except for the one parameter varied, other parameters are kept fixed. Whereas the shear band spacing increases rapidly with an increase in the value of the material characteristic length  $\ell$ , the maximum critical growth rate decreases implying thereby that the consideration of dipolar effects has a stabilizing effect. The shear band spacing for the titanium (Ti) alloy increases from 0.4 mm to 2.50 mm when  $\ell$  is increased from 0 to 0.01. Nesterenko et al. (1995) have measured the spacing between adjacent shear bands formed due to the radial collapse of a thick-walled cylinder at a strain-rate of about  $10^4/s$ . They reported  $L_s = 1$  mm, and values computed with the Wright-Ockendon, Grady-Kipp, and Molinari models are  $L_{WO} = 0.3$  mm,  $L_{GK} = 1.8$  mm,  $L_M = 0.75$  mm (see Nesterenko et al. (1995)). We note that Molinari (1997) ex-

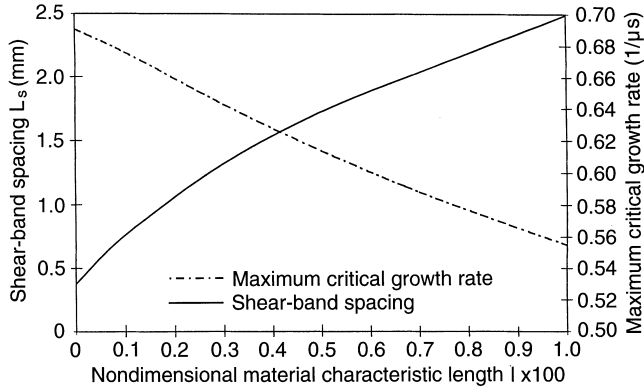


Fig. 3. Dependence of the shear band spacing and the maximum critical growth rate upon the material characteristic length  $\ell$ . Results are for a titanium alloy modeled by the power law

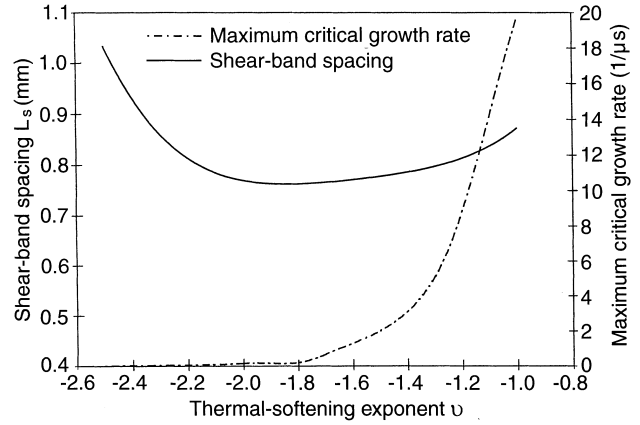


Fig. 6. Shear band spacing and the maximum critical growth rate vs. the thermal softening exponent  $\nu$  for a power-law material

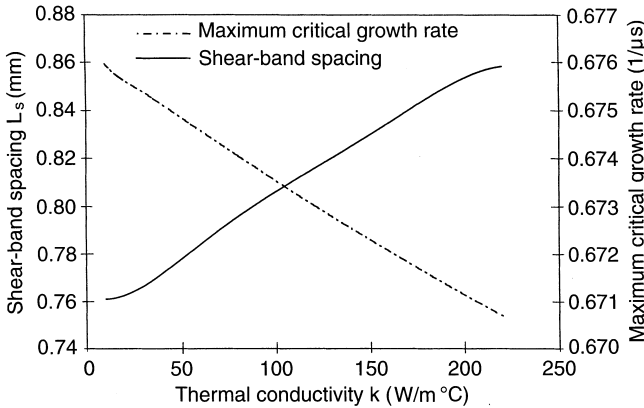


Fig. 4. Variation of the shear band spacing and the maximum critical growth rate with the thermal conductivity for a material modeled by the power law

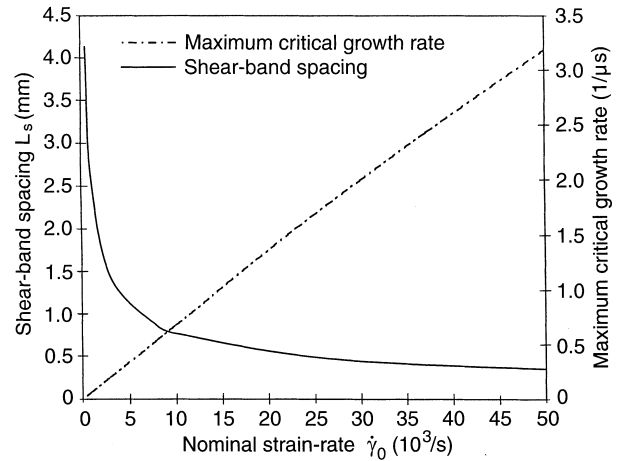


Fig. 7. Shear band spacing and the maximum critical growth rate vs. the nominal strain rate for a power law material

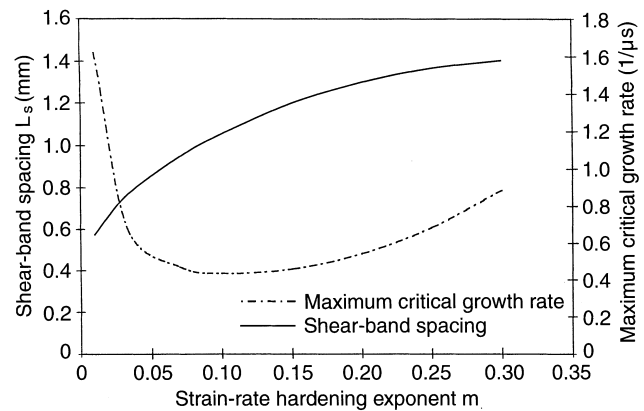


Fig. 5. Shear band spacing and the maximum critical growth rate vs. the strain-rate hardening exponent  $m$  for a power-law material

tended Wright and Ockendon's (1996) work for non-strain hardening materials to strain hardening materials. When strain hardening effects are neglected in Molinari's work, his value of 0.4 mm for  $L_s$  agrees with that obtained here. The value  $L_{W0} = 0.3$  mm is computed from the approximate analytical expression (e.g. see (38)<sub>1</sub> below) derived by Wright and Ockendon. Assuming that values (20) of all

material parameters except for  $\ell$  are correct, then the value of  $\ell$  can be ascertained by matching the computed shear band spacing with the observed value. A real test of the dipolar theory will then be to compare its predictions with the test values for a different configuration; this is not pursued here. Out of the five parameters varied, the maximum critical growth rate is very sensitive to the thermal softening exponent  $\nu$  and the strain-rate hardening exponent  $m$ , and the shear band spacing to the material characteristic length  $\ell$  and the nominal strain-rate  $\dot{\gamma}_0$ . The shear band spacing decreases from 4.2 mm to about 0.3 mm when  $\dot{\gamma}_0$  is increased from 500/s to  $10^5$ /s; for larger values of  $\dot{\gamma}_0$ , the shear band spacing is essentially unaffected. When thermal conductivity is varied in SI units from 10 to 220, the shear band spacing increases from 0.76 mm to 0.86 mm.

### 3.2 Results for SAE 4340 steel modeled by the Wright-Batra relation

We model the thermoviscoplastic response of the material by the Wright-Batra relation, and assign following values, which are typical for a hard steel, to various material and geometric parameters; see Batra and Kim (1990b).

$$\begin{aligned}
H &= 2.5 \text{ mm}, & \dot{\gamma}_0 &= 3300/\text{s}, & \bar{\rho} &= 7860 \text{ kg/m}^3, \\
\bar{k} &= 50 \text{ W/mK}, & \bar{\alpha} &= 0.00185/\text{K}, & \bar{c} &= 473 \text{ J/kgK}, \\
s_0 &= 405 \text{ MPa}, & m &= 0.0117, & \bar{b} &= 10^4 \text{ s}, & \ell &= 0.001.
\end{aligned}
\tag{23}$$

They determined these values by solving numerically an initial-boundary-value problem so that the computed stress-strain curve essentially matched the experimental curve of Marchand and Duffy (1988). They also pointed out that these values are not uniquely determined. Figure 8 shows the initial dominant growth rate vs. the wave number for three different values of  $t_0$ , and Fig. 9 depicts the critical growth rate  $\eta_m$  and the critical wavelength  $L_m$  as a function of  $t_0$  for four different values of the material characteristic length  $\ell$ . Whereas for the previous case, the critical wavelength has a minimum value at  $t_0 = 0$ , for the present case the minima of  $1/\xi_m$  occurs for a rather large value of  $t_0$ . In both cases, the effective stress for the homogeneous solution is maximum at  $t_0 = 0$ . As for the power law material model (9b) considered above, the critical wavelength  $L_m$  increases with an increase in the value of  $\ell$ . For the material model (9b),  $L_m$  takes on a minimum value at  $t_0 = 0$  for all four values of  $\ell$  considered, but for the material model (9a), the value of  $t_0$  when  $L_m$  becomes minimum is different for each value of  $\ell$  considered. Results plotted in Figs. 10 and 11 evince that the shear band spacing and the corresponding time  $t_0^\xi$  (the definition of  $t_0^\xi$  is illustrated in Fig. 9a) increase with an increase in the value of  $\ell$ , and they decrease with an increase in the value of the thermal softening coefficient,  $\alpha$ . A higher value of  $\alpha$  will enhance the thermal softening effect which should result in the formation of shear bands at earlier times. The present computations suggest that the shear band spacing decreases for higher values of  $\alpha$ . We note that for many materials, for example a tungsten heavy alloy,  $\alpha$  is greater than the reciprocal of their melting temperatures.

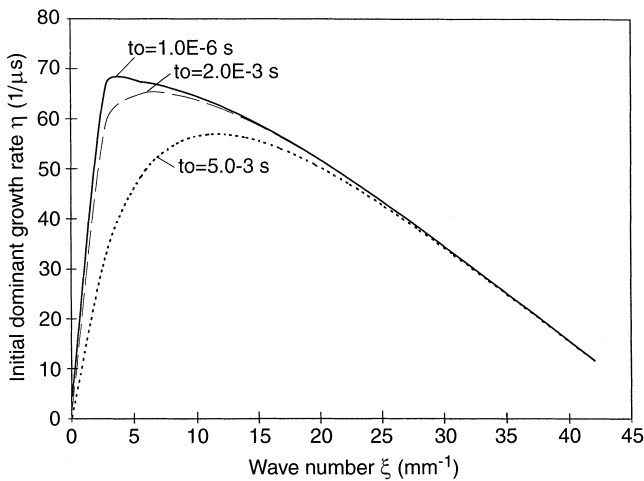


**Fig. 8.** Variation of the initial dominant growth rate vs. the wave number of the perturbation for three different values of the time  $t_0$  when the perturbation is introduced. Results are for a typical hard steel modeled by the Wright-Batra relation with affine thermal softening

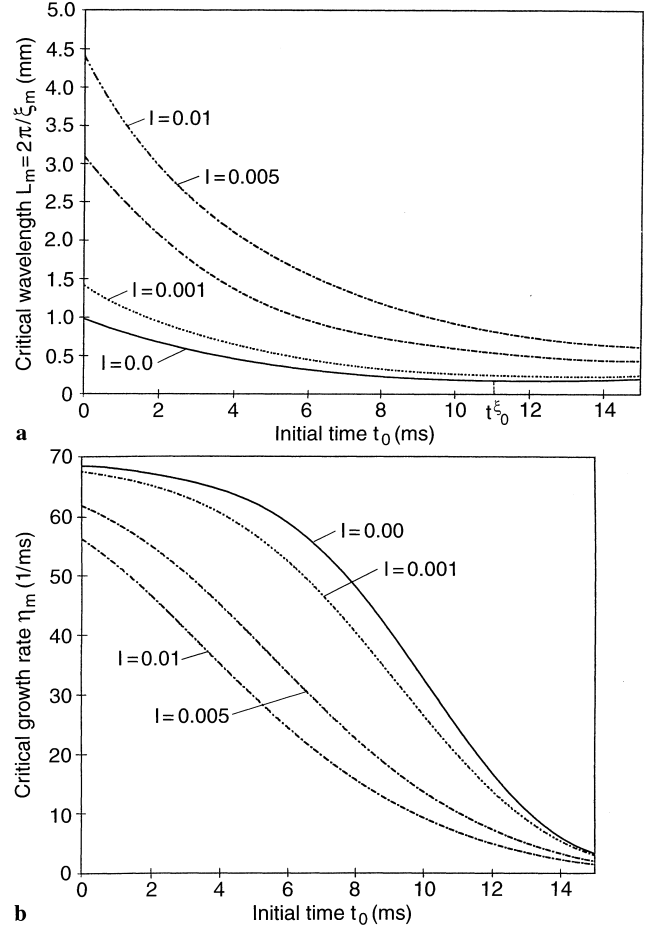


**Fig. 9.** Critical growth rate and the critical wavelength vs.  $t_0$  for four different values of the material characteristic length  $\ell$ . Results are for a typical hard steel modeled by the Wright-Batra relation with affine thermal softening

Figures 12 and 13 exhibit the influence of the strain-rate hardening exponent  $m$  and the thermal conductivity  $k$  upon the shear band spacing and the corresponding initial time,  $t_0^\xi$ . The shear band spacing is maximum for  $m \simeq 0.05$

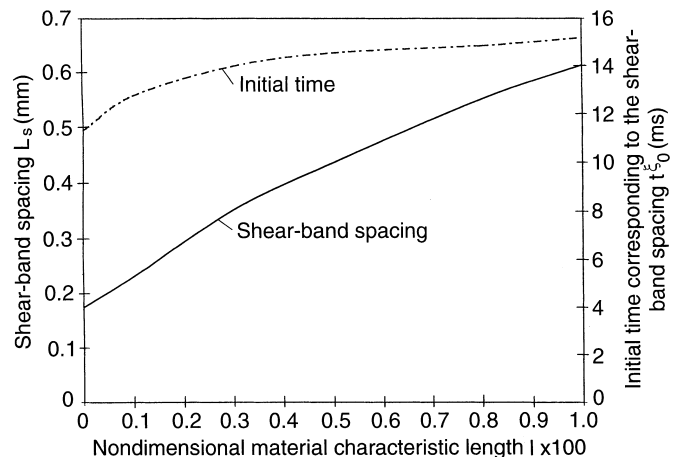


**Fig. 10.** Dependence of the shear band spacing and the corresponding initial time  $t_0^\xi$  upon the material characteristic length  $\ell$  for a typical hard steel modeled by the Wright-Batra relation

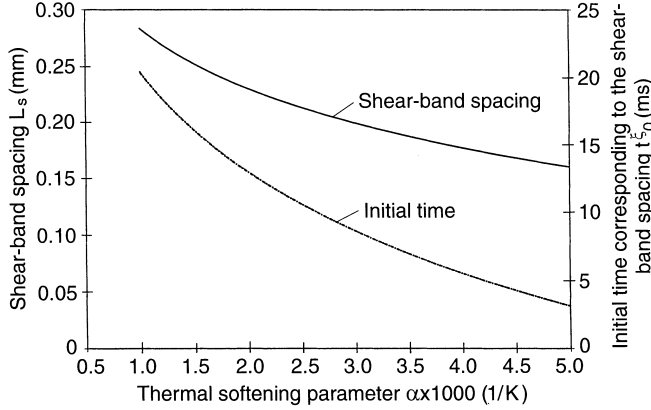


Fig. 11. Shear band spacing and the corresponding initial time  $t_0^\xi$  vs. the thermal softening coefficient  $\alpha$  for the Wright-Batra relation with affine thermal softening

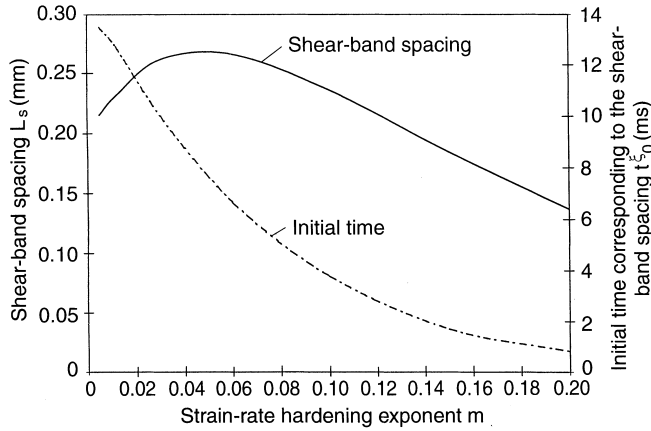


Fig. 12. Shear band spacing and the corresponding initial time  $t_0^\xi$  vs. the strain-rate hardening exponent  $m$  for the Wright-Batra relation with affine thermal softening

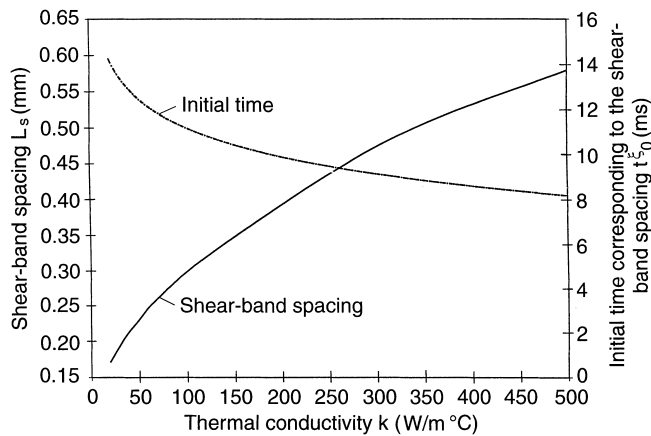


Fig. 13. Variation of the shear band spacing and the corresponding initial time  $t_0^\xi$  with the thermal conductivity for a material modeled by the Wright-Batra relation with affine thermal softening

and equals 0.27 mm. However, the initial time when the perturbation is introduced which leads to the shear band spacing decreases rapidly and monotonically with an increase in the value of  $m$ . Higher values of the thermal

conductivity increase the shear band spacing but decrease the value of the corresponding initial time  $t_0^\xi$ . An increase in the value of the thermal conductivity by a factor of 10 increases the shear band spacing by a factor of nearly 2.5.

Nesterenko et al. (1995) measured the shear band spacing in an austenitic stainless steel to be 0.85 mm. For their material parameters, our analysis gives  $\bar{L}_s = 0.05$  mm for  $\ell = 0$  and  $\bar{L}_s = 0.08$  mm when  $\ell = 0.001$ . For material parameters (23), and  $\ell = 0$ , we get  $\bar{L}_s = 0.18$  mm. Values of shear band spacing obtained from the work of Wright and Ockendon, and Grady and Kip equal 0.314 mm and 5.1 mm respectively. A limitation of Wright and Ockendon's, Molinari's and the present work is that the thickness of the layer is taken to be very large. In a layer of finite thickness, the only admissible instability modes are  $\xi_n = n\pi/H$ ,  $n = 1, 2, \dots$ . Molinari (1997) estimated the relative error in values of the shear band spacing obtained with an infinite layer thickness to be  $\bar{L}_s/2H$ . For our problem, for  $\ell = 0.0$ ,  $\bar{L}_s/2H = 0.036$ . Molinari used a power-law model with strain hardening to characterize the thermoviscoplastic response of the material and obtained  $\bar{L}_s = 1.4$  mm for a hard steel. His value of shear band spacing is quoted for reference only, and does not correspond to material parameters (23). The other two values for the shear band spacing are derived from the approximate expressions given by the authors.

As for the power law model, the shear band spacing decreases rapidly (cf. Fig. 14) with an increase in the value of  $\dot{\gamma}_0$  from 500/s to  $10^5$ /s and is unaffected for higher values of  $\dot{\gamma}_0$ .

Kwon and Batra (1988) assumed that the initial temperature in the block was given by a cosine function with  $\xi = 10\pi/H$ , numerically solved the full nonlinear set of equations with appropriate boundary conditions and also included the effects of strain hardening and material elasticity. For  $\ell = 0$ ,  $\dot{\gamma}_0 = 500$ /s or 50,000/s and  $\alpha = 0.4973$ , they found the spacing between adjacent shear bands to be 0.258 mm. They did not investigate the effect of different amplitudes of the perturbation, the wave number  $\xi$ , and the spatial discretization used to numerically solve the problem. A high value of the thermal softening coefficient,  $\alpha$ , should result in a smaller value of the

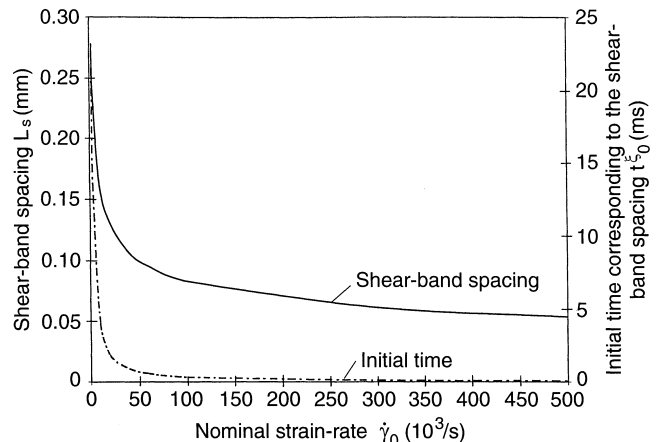


Fig. 14. Shear band spacing and the corresponding initial time  $t_0^\xi$  vs. the nominal strain rate for the Wright-Batra material with affine thermal softening

shear band spacing, but the consideration of strain-hardening should increase the shear band spacing. As stated in the Introduction, the shear bands developed at the troughs of the perturbation for  $\dot{\gamma}_0 = 500/s$  and at the crests for  $\dot{\gamma}_0 = 50,000/s$ . Thus the shear band spacing was the same at these two values of the nominal strain-rate. For  $\ell = 0.01$  shear bands formed at the boundaries  $y = \pm 1$  for  $\dot{\gamma}_0 = 500/s$  but at each peak in the perturbation for  $\dot{\gamma}_0 = 50,000/s$ ; thus  $\bar{L}_s = 5.16$  mm for  $\dot{\gamma}_0 = 500/s$  and 0.258 mm for  $\dot{\gamma}_0 = 50,000/s$ ; this agrees qualitatively with the present results. We note that in Kwon and Batra's work, the shear band spacing is governed by the momentum diffusion during unloading within the shear banded region, the growth of perturbations, the amplitude of initial perturbations, and the effect of boundary conditions. Batra and Kim (1990c) noted that for large values of the thermal softening coefficient,  $\alpha$ , an unloading elastic wave emanated from the shear banded region and propagated outwards with the speed of the shear wave for  $\ell = 0$ , but no such unloading wave originated for  $\ell > 0$ . Results plotted in Fig. 8 indicate that the perturbation introduced at  $t_0 \simeq 0$  with wave number  $\zeta = 10\pi/2.5 \simeq 12.6$  mm<sup>-1</sup> does not have the dominant initial growth rate.

Batra and Kim (1990a) introduced a finite amplitude perturbation with peaks of different magnitudes centered at  $y = \pm 0.02$  and  $y = \pm 0.06$ , numerically solved the full nonlinear set of equations, and also accounted for material elasticity and strain-rate hardening. For  $\ell = 0$  and  $\dot{\gamma}_0 = 500/s$ , the shear band spacing was found to be 0.18 mm when the peaks of higher amplitude were centered at  $y = \pm 0.06$ , and only one shear band with center at  $y = 0$  formed when the peaks of higher amplitude were centered at  $y = \pm 0.02$ . However, when  $\dot{\gamma}_0 = 50,000/s$ , the shear band spacing equalled 0.31 mm in each case. For  $\ell = 0.01$ , only one shear band centered at  $y = 0$  formed for each perturbation and for both values of  $\dot{\gamma}_0$ . These perturbations when expressed as a Fourier series will equal the sum of several perturbations of different wave numbers and amplitudes. The shear band spacing will be determined by the boundary conditions, the growth rate and the amplitudes of various perturbations, and the interaction amongst them. Results from the present linear analysis will not apply to such a case. Also, Batra and Kim (1990a) did not investigate the effect of spatial and temporal discretization upon the shear band spacing.

In the numerical solution of the complete set of nonlinear equations, the boundary conditions at  $y = \pm 1$  and the discretization of the spatial and temporal domains influence the accuracy of the solution. The stability analysis of the linearized equations indicates that for the affine thermal softening, the shear band spacing is determined by the wavelength of the dominant mode of the perturbation introduced at a large value of  $t_0$  when the stress has dropped significantly from its peak value. However, in the numerical work of Kwon and Batra, and Batra and Kim, the perturbations of finite amplitude were introduced essentially at  $t_0 = 0$ . Also, the consideration of material elasticity allows for unloading of a material point and the transfer of energy from the unloading region to other parts of the body; this effect is not included in the present work.

### 3.3 Results for a S-7 tool steel modeled by the Johnson-Cook relation

The tool steel is modeled by the Johnson-Cook relation with

$$s_0 = 1539 \text{ MPa}, \quad C = 0.012, \quad \bar{\rho} = 7750 \text{ kg/m}^3, \\ \bar{\alpha} = 6.8 \times 10^{-4} / \text{K}, \quad \bar{c} = 477 \text{ J/kg K}, \quad \bar{k} = 50 \text{ W/mK}, \\ H = 2.5 \text{ mm}, \quad \dot{\gamma}_0 = 3300/s, \quad \ell = 0.001.$$

Figures 15a and 15b exhibit for four values of  $\ell$  the dependence of the critical wavelength and the critical growth rate upon the time  $t_0$  when the homogeneous solution is perturbed. The results are qualitatively similar to those obtained with the Wright-Batra relation even though strain-rate hardening is now modeled by a different function. For each value of  $\ell$ , the critical wavelength that determines the shear band spacing corresponds to the perturbation given at a rather large value  $t_0$  of time  $t$ . The dependence of the shear band spacing and the time  $t_0^\zeta$  of the perturbation that deter-

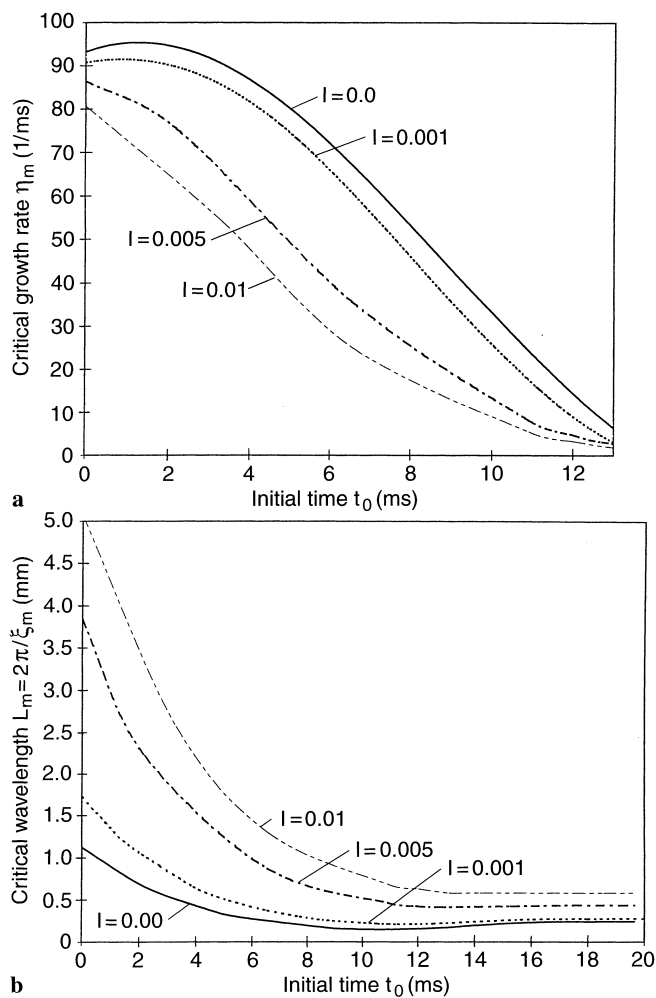


Fig. 15. Dependence of a the critical growth rate and b the critical wavelength upon the time  $t_0$  when the initial perturbation is introduced for four different values of the material characteristic length  $\ell$ . Results are for a typical hard steel modeled by the Johnson-Cook relation

mines the shear band spacing upon the material characteristic length  $\ell$ , thermal softening parameter  $\alpha$ , strain-rate hardening parameter  $C$ , the thermal conductivity  $k$ , and the nominal strain-rate  $\dot{\gamma}_0$  is similar to that for the Wright-Batra relation. For  $\ell = 0$ , the shear band spacing,  $\bar{L}_s$ , equals 0.15 mm, and it monotonically increases to 0.57 mm for  $\ell = 0.01$ . When the thermal softening parameter  $\bar{\alpha}$  is increased from 0.0005/K to 0.005/K,  $\bar{L}_s$  decreases from 0.23 mm to 0.11 mm. A change in the value of  $C$  from 0.01 to 0.05 increases the shear band spacing from 0.196 mm to 0.26 mm. A ten-fold increase in  $\bar{k}$  from 50 W/mK to 500 W/mK increases the shear band spacing from 0.21 mm to 0.5 mm. When the nominal strain-rate is increased from 2000/s to 50,000/s, the shear band spacing decreases from 0.24 mm to 0.03 mm.

#### 4

##### Approximate analytical expressions for shear band spacing

In the previous section we have numerically evaluated the shear band spacing. It was found that for  $t_0 \geq 0$  and a given wave number  $\xi$ , there always exists a root of (17) with a positive real part. Also, the root  $\eta_m$  of (17) with the maximum positive real part was found to be a function of the wave number  $\xi_m(t_0)$  and the initial time  $t_0$  when the perturbation was introduced. Thus  $\eta_m$  should satisfy

$$\left. \frac{\partial \eta(\xi, t_0)}{\partial \xi} \right|_{\xi=\xi_m} = 0. \quad (24)$$

Differentiating (17) with respect to  $\xi$ , evaluating the result at  $\xi = \xi_m$ , and substituting (24) we arrive at

$$\bar{a}_{1m}\eta_m + \bar{a}_{0m} = 0 \quad (25)$$

where

$$\bar{a}_{\beta m} = \left. \frac{\partial a_{\beta m}(\xi, t_0)}{\partial \xi} \right|_{\xi=\xi_m}, \quad \beta = 0, 1. \quad (26)$$

Evaluating (17) at  $(\xi, \eta) = (\xi_m, \eta_m)$  and eliminating  $\eta_m$  from it and (25), we obtain

$$a_2(\bar{a}_{0m})^2 - a_{1m}\bar{a}_{0m}\bar{a}_{1m} + a_{0m}(\bar{a}_{1m})^2 = 0 \quad (27)$$

where

$$a_{\beta m} = a_{\beta}(\xi_m, t_0), \quad \beta = 0, 1. \quad (28)$$

Substitution from (18) into (26) and (28), and the results into (27) yields

$$b_{10}\xi_m^{10} + b_8\xi_m^8 + b_6\xi_m^6 + b_4\xi_m^4 + b_2\xi_m^2 + b_0 = 0 \quad (29)$$

where

$$\begin{aligned} b_{10} &= 8k(\ell^2 s^0 f_s^0)^3, \\ b_8 &= (\ell^2 s^0 f_s^0)^2 (-36\rho k^2 f_s^0 + 20k(1 + \rho k f_s^0)), \\ b_6 &= -24\rho \ell^2 k s^0 (f_s^0)^2 (k + \ell^2 s^0 f_\theta^0) \\ &\quad + 8\ell^2 s^0 f_s^0 (1 + \rho k f_s^0) (k + \ell^2 s^0 f_\theta^0) \\ &\quad + 24\rho k f_\theta^0 (\ell^2 s^0 f_s^0)^2 + 8\ell^2 k s^0 f_s^0 (1 + \rho k f_s^0)^2 \\ &\quad + 16s^0 f_\theta^0 (\ell^2 s^0 f_\theta^0)^2, \end{aligned}$$

$$\begin{aligned} b_4 &= 24\rho k f_\theta^0 (\ell s^0 f_s^0)^2 - 16\rho f_s^0 (k + \ell^2 s^0 f_\theta^0)^2 \\ &\quad + 8\ell^2 (s^0)^2 f_s^0 f_\theta^0 (1 + \rho k f_s^0) \\ &\quad + 16\rho \ell^2 s^0 f_s^0 f_\theta^0 (k + \ell^2 s^0 f_\theta^0) \\ &\quad + 12\rho \ell^2 k s^0 f_s^0 f_\theta^0 (1 + \rho k f_s^0) \\ &\quad + 8(k + \ell^2 s^0 f_\theta^0) (1 + \rho k f_s^0)^2, \\ b_2 &= 16\rho s^0 f_s^0 f_\theta^0 (k + \ell^2 s^0 f_\theta^0) - 8s^0 f_\theta^0 (\ell^2 s^0 f_s^0)^2 \\ &\quad - 8\rho f_s^0 (\ell s^0 f_\theta^0)^2 + 8\rho f_\theta^0 (1 + \rho k f_s^0) (k + \ell^2 s^0 f_\theta^0), \\ b_0 &= -4\rho f_s^0 (s^0 f_\theta^0)^2 - 4(\ell s^0)^2 f_s^0 f_\theta^0 (1 + \rho k f_s^0) \\ &\quad - 4\rho s^0 (f_\theta^0)^2 (1 + \rho k f_s^0) \end{aligned} \quad (30)$$

Equation (29) determines the critical wave number  $\xi_m$  as a function of the time  $t_0$  when the perturbation is introduced; it has been assumed here that the root  $\eta_m$  of (25) corresponds to a maxima. Setting the derivative of (29) with respect to  $t_0$  equal to zero determines  $t_0^\xi$  corresponding to an extreme value  $\xi_{mm}$  of  $\xi_m$ , which we assume to be maximum. The maximum value  $\xi_{mm}$  of  $\xi_m$  determines the shear band spacing corresponding to the time  $t_0^\xi$ . Because of the complicated algebraic manipulations involved, an analytical expression for  $\xi_{mm}$  is not found here.

From (25) we can ascertain the critical growth rate,  $\eta_m$ , as

$$\eta_m = \frac{-3\ell^2 k s^0 f_s^0 \xi_m^4 - 2(k + \ell^2 s^0 f_\theta^0) \xi_m^2 + s^0 f_\theta^0}{2\ell^2 s^0 f_s^0 \xi_m^2 + (1 + \rho k f_s^0)} \quad (31)$$

Using the constitutive relation (9a), the homogeneous solution (10a), noting that  $\ell \ll 1$ , determining the magnitudes of different terms, and keeping only dominant terms, we obtain the following explicit expressions for the critical wave number  $\xi_m$  and the critical growth rate  $\eta_m$  of the dominant instability mode.

$$\xi_m = [(-P + \sqrt{P^2 - 4QR})/2Q]^{1/2}, \quad (32)$$

$$\eta_m = [-2(k + \alpha \ell^2 b^m / m) \xi_m^2 + \alpha b^m / m] / (1 + \rho k e^{\Gamma t_0} / m b^m), \quad (33)$$

where

$$\begin{aligned} Q(t_0) &= -\left(k + \frac{\alpha \ell^2 b^m}{m}\right) \left[ \frac{4\rho \alpha \ell^2 e^{\Gamma t_0}}{m^2} - \left(1 - \frac{\rho k e^{\Gamma t_0}}{m b^m}\right)^2 \right] \\ &\quad + \frac{\alpha \ell^2 b^m}{m^2}, \\ P(t_0) &= \frac{2\rho \alpha}{m^2} \left(2 + \frac{\rho k e^{\Gamma t_0}}{b^m}\right) \left(k + \frac{\alpha \ell^2 b^m}{m}\right) e^{\Gamma t_0}, \\ R(t_0) &= -\frac{\rho \alpha^2 b^m}{m^3} \left(1 + \frac{\rho k e^{\Gamma t_0}}{b^m}\right) e^{\Gamma t_0}. \end{aligned} \quad (34)$$

For the constitutive relation (9b) and the homogeneous solution (10b), expressions analogous to (31) and (34) are

$$\eta_m = \frac{-3 \frac{\ell^2 k \zeta_m^4}{m} - 2 \left( k - \frac{\ell^2 v \mu_0}{m} (\theta^0)^{v-1} \right) \zeta_m^2 - \frac{v \mu_0}{m} (\theta^0)^{v-1}}{\frac{2 \ell^2}{m} \zeta_m^2 + \left( 1 + \frac{\rho k}{m \mu_0} (\theta^0)^{-v} \right)}, \quad (35)$$

$$Q(t_0) = \left( k - \frac{\ell^2 \mu_0 v}{m} (\theta^0)^{v-1} \right) \times \left[ \frac{4 \ell^2 \rho v}{m^2 \mu_0} (\theta^0)^{-(1+v)} + \left( 1 - \frac{\rho k}{m \mu_0} (\theta^0)^{-v} \right)^2 \right] - \frac{\ell^2 \mu_0 v}{m^2} (\theta^0)^{v-1},$$

$$P(t_0) = -\frac{2 \rho v}{m^2 \mu_0} (\theta^0)^{-(1+v)} \left[ k - \frac{\ell^2 \mu_0 v}{m} (\theta^0)^{v-1} \right] \times [2 \mu_0 (\theta^0)^v + \rho k], \quad (36)$$

$$R(t_0) = -\frac{\rho \mu_0 v^2}{m^3} (\theta^0)^{v-2} \left[ 1 + \frac{\rho k}{\mu_0} (\theta^0)^{-v} \right].$$

For the Johnson-Cook model (9c) and the homogeneous solution (10c), equations (33) and (34) become

$$\eta_m = \frac{-3 \ell^2 k A \zeta_m^4 - 2(kC + \alpha \ell^2 A^2) \zeta_m^2 + \alpha A^2}{2 \ell^2 A \zeta_m^2 + (C + \rho k e^{\alpha A t_0})}, \quad (37)$$

$$Q(t_0) = \left( \frac{k}{C^2} + \frac{\alpha \ell^2 A^2}{C^3} \right) \times [-4 \rho \ell^2 \alpha A e^{2\alpha A t_0} + (C - \rho k e^{\alpha A t_0})^2] + \frac{\alpha \ell^2 A^3}{C^4},$$

$$P(t_0) = \frac{2 \rho \alpha A}{C^3} e^{2\alpha A t_0} (Ck + \ell^2 \alpha A^2) (\rho k + 2A e^{-\alpha A t_0}), \quad (38)$$

$$R(t_0) = -\frac{\rho \alpha^2 A^3}{C^3} e^{\alpha A t_0} [C + A + \rho k e^{\alpha A t_0}].$$

Figures 16a, 16b and 16c exhibit the variation with  $t_0$  of the critical wavelength and the critical growth rate as computed from (32)–(34), (32), (35) and (36), and (32), (37) and (38), which correspond to the Wright-Batra relation, the power law, and the Johnson-Cook relation, respectively. Also included are numerical results from the previous section. It is clear that the two sets of results are close to each other signifying that the approximate expressions (32)–(34), (32), (35) and (36), and (32), (37) and (38) can be used with reasonable certainty. The shear band spacing can be computed from (32).

For nonpolar ( $\ell = 0$ ) materials, the (dimensional) critical wavelength computed from  $2\pi/\zeta_m$  is given by

$$\bar{L}_m/2\pi = \begin{cases} \left( \frac{m^3 \bar{k} \bar{c} (1 - \bar{\alpha} \bar{\theta}_i)}{(1+m) \dot{\gamma}_0^3 \bar{s}^2 \bar{s}^0} \right)^{1/4} & \text{for the Wright-Batra relation,} \\ \left( \frac{m^3 (\bar{\theta}_i)^2 \bar{c} \bar{k}}{(1+m) \dot{\gamma}_0^3 \bar{s}^0 v^2} \right)^{1/4} & \text{for the power law,} \\ \left( \frac{C^3 \bar{k} \bar{c} (1 - \bar{\alpha} \bar{\theta}_i)}{\bar{\alpha}^2 \dot{\gamma}_0^3 (1+C \ln \dot{\gamma}_0)^3 \bar{s}^0} \right)^{1/4} & \text{for the Johnson-Cook relation} \end{cases} \quad (39)$$

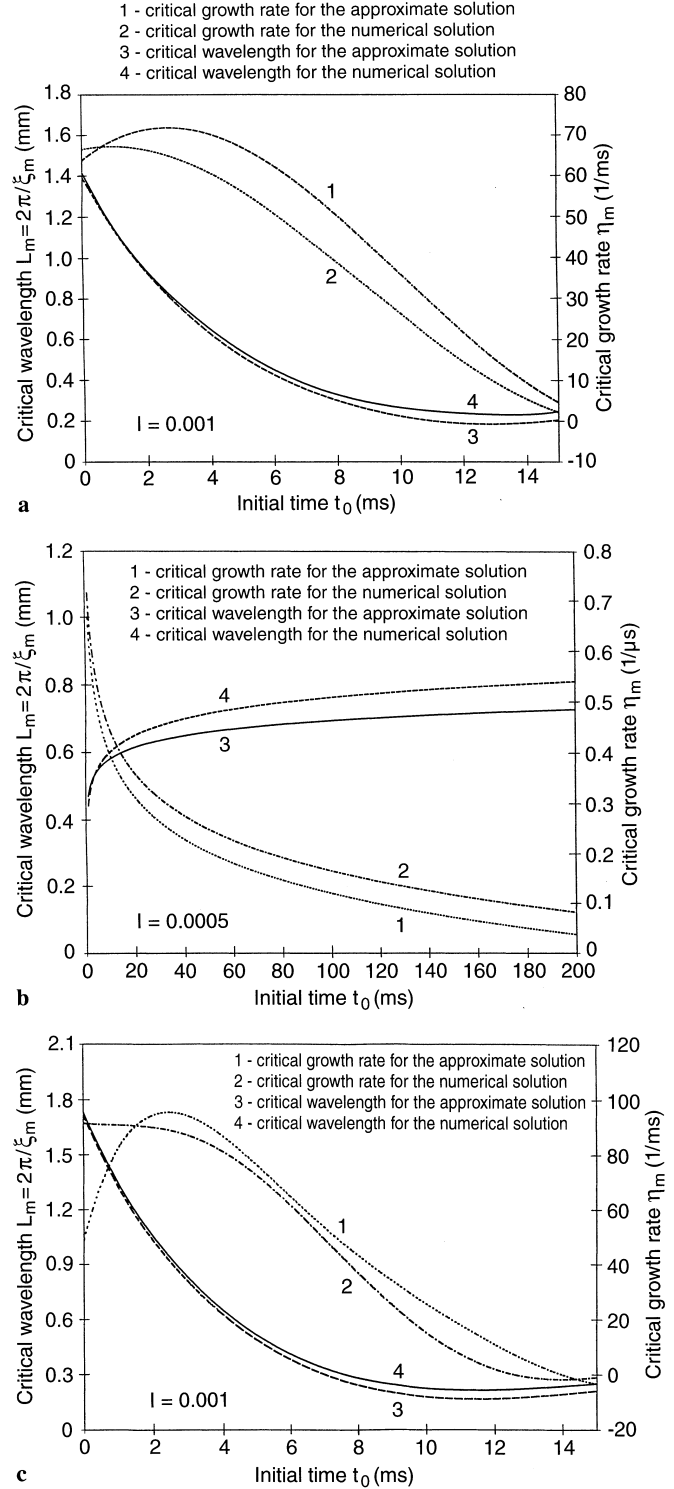


**Fig. 16.** Dependence of the critical wavelength and the critical growth rate upon the time  $t_0$  when the perturbation is introduced; a power law, b Wright-Batra relation with affine thermal softening, and c Johnson-Cook model

where we have assumed that  $\rho k \ll m s^0$ , set  $\bar{s}^0 = s_0 (\bar{b} \dot{\gamma}_0)^m$  for the Wright-Batra relation, and  $\bar{s}^0 = s_0 (1 + C \ln \dot{\gamma}_0)$  for the Johnson-Cook relation, and  $\bar{\theta}_i$  equals the value of  $\bar{\theta}^0$  at time  $t_0$ . Expression (39)<sub>1</sub> for the critical wavelength differs from that derived by Wright and Ockendon in the factor  $(1 - \bar{\alpha} \bar{\theta}_i)$  in the numerator. Wright and Ockendon

used a different method to derive their approximate expression for  $\bar{L}_s$ . However, our results (39)<sub>1</sub> and (39)<sub>2</sub> agree with those of Molinari (1997). As also pointed out by Molinari,  $(1 - \bar{\alpha}\bar{\theta}_i)$  can be quite different from 1.0. For an affine thermal softening, it is likely that the condition  $\rho k \ll ms^0$  will be violated for  $t_0$  corresponding to the supremum of  $\xi_m(t_0)$ . Nevertheless, (39) gives the critical wavelength whenever  $\rho k \ll ms^0$  holds. A comparison of (39)<sub>1</sub> and (39)<sub>3</sub> suggests that  $C/(1 + C \ln \dot{\gamma}_0)$  plays the same role as the strain-rate hardening exponent  $m$ . For each material model, the approximate value of the critical wavelength is independent of the mass density of the material, increases rapidly with an increase in the strain-rate hardening exponent  $m$ , decreases fast with an increase in the average strain-rate, and decreases with a rise in the thermal softening coefficient  $\alpha$  or exponent  $\nu$ . In determining the shear band spacing, the thermal softening exponent  $\nu$  in the power law plays the same role as the thermal softening coefficient  $\alpha$  in the other two constitutive relations.

The minimum value of  $\bar{L}_m$  in (39) will give the shear band spacing. When thermal softening is modeled by an affine function of temperature,  $\bar{\theta}_i$  will be maximum for a large value of the time  $t_0$  when a perturbation is introduced, and  $(1 - \bar{\alpha}\bar{\theta}_i)$  may equal zero. In this case, the minimum shear band spacing equals zero. Of course, the numerical solution of the complete set of equations gives a finite value of the shear band spacing. For the power law model, the minimum shear band spacing occurs when the homogeneous solution of the governing equations is perturbed at time  $t_0 = 0$ . These observations are in conformity with the numerical experiments described above.

We note that even the trends predicted by (39) need not agree with those obtained from a solution of (17). For example, the shear band spacing plotted in Fig. 12 for the Wright-Batra relation is maximum at  $m \simeq 0.05$  and then monotonically decreases with an increase in the value of  $m$ . However, (39)<sub>1</sub> indicates that it is a monotonically increasing function of  $m$  since  $1 + m \simeq 1$ .

A reasonable postulate is that for  $L_s > 0$ , the band-width is a fraction of the shear band spacing. Dodd and Bai (1985) assumed that in a fully developed band, heat generated due to plastic working is balanced by that conducted out of the band. They showed that the band-width is proportional to the square-root of the thermal conductivity and is independent of the specific heat of the material. However, the shear band spacing given by (39) depends upon  $(\bar{k}\bar{c})^{1/4}$ . Numerical experiments of Batra and Kim (1991) suggest that the band-width is not proportional to  $\sqrt{k}$ . Batra and Kim (1992) also obtained different band-widths for three steels with the same thermal conductivity suggesting that other material parameters strongly influence the band-width.

Within a shear band, plastic strain-rates are usually very high and because heat conduction is a slow process, there may not be enough time available for the heat to be conducted out of the bands. The process of shear band formation is often regarded as locally adiabatic. For  $k = 0$ , the critical wave number,  $\xi_m$ , and the critical wavelength,  $\bar{L}_m$ , are given by

$$\xi_m^2 = \sqrt{\rho f_{,0}^0} / \ell, \quad (40)$$

$$\bar{L}_m / 2\pi = \begin{cases} \left( \frac{\bar{\ell}}{\dot{\gamma}_0} \right)^{\frac{1}{2}} \left( \frac{m(1-\bar{\alpha}\bar{\theta}_0)\bar{c}}{\bar{\alpha}} \right)^{\frac{1}{4}} & \text{for the Wright-} \\ & \text{Batra relation,} \\ \left( \frac{\bar{\ell}}{\dot{\gamma}_0} \right)^{\frac{1}{2}} \left( -\frac{\bar{c}\bar{\theta}_i m}{\nu} \right)^{\frac{1}{4}} & \text{for the} \\ & \text{power law,} \\ \left( \frac{\bar{\ell}}{\dot{\gamma}_0} \right)^{\frac{1}{2}} \left[ \frac{\bar{c}C(1-\bar{\alpha}\bar{\theta}_0)}{\bar{\alpha}(1+C \ln \dot{\gamma}_0)} \right]^{\frac{1}{4}} & \text{for the} \\ & \text{Johnson-Cook law .} \end{cases} \quad (41)$$

Thus for each one of the three constitutive relations,  $\bar{L}_m$  is proportional to the square-root of the material characteristic length,  $\bar{\ell}$ , the fourth-root of the strain-rate sensitivity parameter,  $m$  or  $C/(1 + C \ln \dot{\gamma}_0)$ , and inversely proportional to the square-root of the nominal strain-rate,  $\dot{\gamma}_0$ . For heat conducting nonpolar materials,  $\bar{L}_m$  is proportional to  $(m/\dot{\gamma}_0)^{3/4}$ .

## 5 Conclusions

We have ascertained shear band spacing in a thermoviscoplastic body deformed in simple shear, have delineated the effect of different material parameters on the shear band spacing, and have generalized Wright and Ockendon's work on nonpolar (simple) materials to dipolar materials. It entails perturbing the homogeneous solution of the governing equations, linearizing the governing equations in the perturbed variables, and studying the stability of the linearized problem. For a fixed value of the time  $t_0$  when the perturbation is introduced, the maximum wave number and maximum initial growth rate of the perturbation are found. The shear band spacing is assumed to equal the infimum of  $2\pi/\xi_m(t_0)$  for  $t_0 \geq 0$ . Three constitutive relations, namely, the Wright-Batra relation, the power law, and the Johnson-Cook law are used to model the thermoviscoplastic response of the material. The Wright-Batra and the Johnson-Cook models differ in the way strain-rate hardening of the material is accounted for. The Wright-Batra and the power law models characterize the thermal softening of the material by different functions of temperature. It is found that for the power law, perturbations introduced just after the stress becomes maximum determine the shear band spacing. However, for the Wright-Batra and the Johnson-Cook relations in which thermal softening is modeled by an affine function of temperature, the critical wave number increases rather slowly with an increase in the value of the time  $t_0$  when the perturbation is introduced. Thus perturbations introduced at a rather large value of  $t_0$  determine the shear band spacing. The thermal softening exponent/coefficient, the material characteristic length, and the nominal strain-rate noticeably influence the shear band spacing. The shear band spacing so obtained does not agree with that computed from a numerical solution of the complete set of nonlinear equations in which the effects of material elasticity, strain hardening, boundary conditions and perturbations of finite amplitude introduced at time  $t_0$  are considered. In the later case, the wave number of the perturbation was kept fixed.

For locally adiabatic deformations of a nonpolar thermoviscoplastic material,  $k = 0$ ,  $\ell = 0$ . Equations (17) and (18) imply that the initial growth rate,  $\eta$ , is a monotonically increasing function of the wavenumber,  $\zeta$ . According to the definition (22), the shear band spacing equals zero irrespective of the constitutive relation used to model the thermoviscoplastic response of a non-strain-hardening material.

Approximate expressions are derived for the critical wavelength and the critical growth rate of the perturbation. Results computed from these approximate expressions are in reasonable agreement with those obtained from the numerical solution of the complete set of equations linearized in perturbation variables about an homogeneous solution. These approximate expressions for the shear band spacing reveal that the strain-rate hardening exponent,  $m$ , in the power law plays the same role as  $C/(1 + C \ln \dot{\gamma}_0)$  in the Johnson-Cook relation. Also, the thermal softening exponent  $\nu$  in the power law and the thermal softening coefficient  $\bar{\alpha}$  in the Wright-Batra and Johnson-Cook relations play analogous roles. For each one of the three constitutive relations, the approximate shear band spacing for nonpolar materials is found to be proportional to  $\left(\frac{m^3 \bar{k} \bar{c}}{\dot{\gamma}_0^2 \bar{\alpha}^2}\right)^{1/4}$  where  $\bar{k}$ ,  $\bar{c}$  and  $\dot{\gamma}_0$  are the thermal conductivity, specific heat and the nominal strain-rate. However, for locally adiabatic deformations of dipolar materials, the shear band spacing is proportional to  $\left(\frac{\bar{\ell}}{\dot{\gamma}_0}\right)^{1/2} \left(\frac{m \bar{c}}{\bar{\alpha}}\right)^{1/4}$  where  $\bar{\ell}$  is the material characteristic length.

For a nominal strain-rate of  $10^5/s$ , the shear band spacing in Titanium, SAE4340 steel and S-7 tool steel equals respectively 0.25 mm, 0.086 mm, and 0.1 mm. The shear band spacing should serve as an upper limit on the band width. Thus the width of shear bands in Titanium, SAE4340 steel and the S-7 tool steel is likely to be less than 250  $\mu\text{m}$ , 86  $\mu\text{m}$ , and 100  $\mu\text{m}$  respectively.

## References

- Armstrong R, Batra RC, Meyers M, Wright TW (Eds.) 1994: Shear Instabilities and Viscoplastic Theories, Special Vol. of the Mechanics of Materials 17:83–328
- Bai YL, Dodd B (1992) Adiabatic Shear Localization: Occurrence, Theories and Applications, Pergamon, Oxford
- Batra RC, Zbib, HM (Eds.) 1994: Material Instabilities, ASME Press, New York
- Batra RC, Hwang J (1994) Dynamic shear band development in dipolar thermoviscoplastic materials. *Comp. Mech.* 14:354–369
- Batra RC, Kim CH (1992) Analysis of shear bands in twelve materials. *Int. J. Plasticity* 8:425–452
- Batra RC, Kim KH (1991) Effect of thermal conductivity on the initiation, growth and bandwidth of adiabatic shear bands. *Int. J. Engng. Sci.* 29:949–960
- Batra RC, Liu DS (1990) Adiabatic shear band development in dynamic plane strain compression of a viscoplastic material. *Int. J. Plasticity* 6:231–246
- Batra RC, Kim CH (1990a) The interaction among adiabatic shear bands in simple and dipolar materials. *Int. J. Engng. Sci.* 28:927–942
- Batra RC, Kim CH (1990b) Effect of viscoplastic flow rules on the initiation and growth of shear bands at high strain rates. *J. Mech. Phys. Solids* 38:859–874
- Batra RC, Kim CH (1990c) Adiabatic shear banding in elastic-viscoplastic nonpolar and dipolar materials. *Int. J. Plasticity* 6:127–141
- Dodd B, Bai Y (1985) Width of adiabatic shear bands. *Mat. Sci. & Tech.* 1:38
- Green AE, McInnis BC, Naghdi PM (1968) Elastic-plastic continua with simple force dipole. *Int. J. Engng. Sci.* 1:373–394
- Johnson GR, Cook WH (1983) In Proc. 7th Int. Symp Ballistics, The Hague, The Netherlands. 1
- Kwon YW, Batra RC (1988) Effect of multiple initial imperfections on the initiation and growth of adiabatic shear bands in nonpolar and dipolar materials. *Int. J. Engng. Sci.* 26:1177–1187
- Marchand A, Duffy J (1988) An experimental study of the formation process of adiabatic shear bands in a structural steel. *J. Mech. Phys. Solids* 36:251
- Molinari A (1997) Collective behavior and spacing of adiabatic shear bands. *J. Mech. Phys. Solids* 45:9, 1551–1575
- Nesterenko VF, Meyers MA, Wright TW (1995) Collective behavior of shear bands. In *Metallurgical and Materials Application of Shock-Wave and High-Strain-Rate Phenomena*, (Eds.: L. E. Murr, K. P. Staudhammer and M. A. Meyers), Elsevier Science B.V. 397–404
- Perzyna PV (Ed.) 1998: Localization and Fracture Phenomena in Inelastic Solids. Springer-Verlag, Berlin
- Tomita Y (1994) Simulation of plastic instabilities in solid mechanics. *Appl. Mech. Revs.* 47:171–205
- Wright TW, Ockendon H (1996) A scaling law for the effect of inertia on the formation of adiabatic shear bands. *Int. J. Plasticity* 12:927–934
- Wright TW, Batra RC (1987) Adiabatic shear bands in simple and dipolar plastic materials. (Kawata, K. and Shiori, J., eds.) *Macro- and Micro-Mechanics of high velocity deformation and fracture*. IUTAM Symp. on MMMHVDF, Tokyo, Japan, Springer-Verlag, Berlin, Heidelberg. 189–201